Process Biochemistry 48 (2013) 103–108

Contents lists available at SciVerse ScienceDirect

Process Biochemistry

journal homepage: www.elsevier.com/locate/procbio

Elimination of substrate inhibition of a β-*N*-acetyl-D-hexosaminidase by single site mutation

Tian Liu, Qingyue Wu, Lin Liu, Qing Yang*

School of Life Science and Biotechnology, Dalian University of Technology, Dalian 116024, China

ARTICLE INFO

Article history:
Received 13 September 2012
Received in revised form
15 November 2012
Accepted 27 November 2012
Available online 6 December 2012

Keywords:
Chitin
Glucosamine
Hexosaminidase
Insect
Substrate inhibition

ABSTRACT

Substrate inhibition hinders chitinolytic β-*N*-acetyl-D-hexosaminidases in producing *N*-acetyl-D-glucosamine (GlcNAc), the valuable chemical widely applied in medical and food industries. Here we focused on a promising chitinolytic enzyme, OfHex1 from the insect, *Ostrinia furnacalis*. By structural analysis of OfHex1, five residues nearby the active pocket including V327, E328, Y471, V484 and W490 were chosen and nine mutants including V327G, E328Q, E328A, Y471V, V484R, W490A, W490H, V327G/V484R/W490A and V327G/Y471V/W490H were constructed and recombinantly expressed in *Pichia pastoris*. The best-performing mutant, W490A, obtained by a higher yield of 5 mg/L, did not show substrate inhibition even when 5 mM of the substrates, $(GlcNAc)_{2-4}$, were applied. The k_{cat}/K_m values for $(GlcNAc)_{2-4}$ are 239.8, 111.3 and 79.8 s^{-1} mM^{-1}, respectively. Besides, the pH stability of the mutant ranges from pH 4 to 11 and the thermal stability is up to 50 °C. This work suggests the W490A mutant might be an ideal biocatalyst for GlcNAc production from chitin.

1. Introduction

Chitin is the second most abundant biopolymers next to cellulose in nature. There are more than 100 billion tons of raw chitin materials produced on earth annually [1]. The building block of chitin is a monosaccharide derivative of glucose, *N*-acetyl-D-glucosamine (GlcNAc), which has broad applications as therapeutic agents in preventing joint disorders [2], treating inflammatory bowel disease [3], and as nutritional supplements and cosmetic additives [4,5].

Enzymatic hydrolysis of chitin to produce GlcNAc is promising in terms of environmental compatibility and reproducibility [6–8]. The enzyme, glycosyl hydrolase family 20 (GH20) β-*N*-acetyl-D-hexosaminidase (EC 3.2.1.52), is responsible for catalyzing the release of GlcNAc from chitooligosaccharides, the intermediates of chitin degradation catalyzed by chitinase (EC 3.2.1.14). Besides, since chitinase is inhibited by its products chitooligosaccharides [9], β-*N*-acetyl-D-hexosaminidase also plays a role in eliminating chitinase's product inhibition so as to improve the overall efficiency of chitin degradation.

OfHex1 is a chitinolytic β-*N*-acetyl-D-hexosaminidase from the insect *Ostrinia furnacalis* and has been successfully cloned and expressed with high yield in the yeast strain, *Pichia pastoris* [10,11]. Compared to the widely applied microbial β-*N*-acetyl-D-hexosaminidases, OfHex1 with the k_{cat}/K_m value of 3428 s^{-1} mM^{-1} for $(GlcNAc)_2$ is by far the most efficient chitinolytic enzyme (BRENDA database, http://www.brenda-enzymes.info/) [12]. However, OfHex1 as well as many other chitinolytic β-*N*-acetyl-D-hexosaminidases encounters substrate inhibition that hinders its application in industries.

Substrate inhibition is the phenomenon that a certain enzyme does not obey the typical hyperbolic Michaelis–Menten curve, but runs a velocity curve that rises to a maximum and then declines as substrate concentrate increases [13]. This phenomenon has been well documented for estimated 20% of all known enzymes. Although substrate inhibition are linked to diverse physiological functions of the enzymes through the mechanism known as allosteric effects, it has been found to be an obstacle for industrial application of these enzymes [13,14].

As for glycosyl hydrolase, two mechanisms have been proposed for substrate inhibition [15]. The first one is 'transglycosylation mechanism' and the other one is 'second substrate binding mechanism'. For the former, the products of glycoside hydrolase can re-react with substrate to enlighten the sugar chain, causing the apparent decline in reaction velocity. For example, $(GlcNAc)_{5-6}$ can be obtained by incubating $(GlcNAc)_{3-4}$ with the

Abbreviations: GH20, glycosyl hydrolase family 20; GlcNAc, *N*-acetyl-D-glucosamine; HsHex, β-*N*-acetyl-D-hexosaminidase from human placenta; MU-β-GlcNAc, 4-methylumbelliferyl-*N*-acetyl-β-D-glucosaminide; OfHex1, β-*N*-acetyl-D-hexosaminidase from *Ostrinia furnacalis*; *p*NP-β-GlcNAc, *p*-nitrophenyl-*N*-acetyl-β-D-glucosamine; SmChb, chitobiase from *Serratia marcescens*; SpHex, β-*N*-acetyl-D-hexosaminidase from *Streptomyces plicatus*.

* Corresponding author at: No. 2 Linggong Road, Dalian 116024, China.
Tel.: +86 411 84707245; fax: +86 411 84707245.
E-mail address: qingyang@dlut.edu.cn (Q. Yang).

1359-5113/$ – see front matter © 2012 Elsevier Ltd. All rights reserved.
http://dx.doi.org/10.1016/j.procbio.2012.11.018

β-*N*-acetyl-D-hexosaminidase from fungus *Aspergillus oryzae* [16]. The "second substrate binding" mechanism means that there is more than one substrate binding at the substrate binding site of an enzyme. Thus, the second substrate molecule can act as an allosteric inhibitor. The substrate inhibition of β-*N*-acetyl-D-hexosaminidase from *Penicillium oxalicum* by high concentration of the synthesized substrate, *p*-nitrophenyl-*N*-acetyl-β-D-glucosamine (*p*NP-β-GlcNAc), was well identified by the secondary binding site of the active pocket [17].

Here, we clarified the substrate inhibition mechanism of OfHex1. Based on crystal structure analysis, site-directed mutagenesis of amino acid residues nearby the active pocket was performed to eliminate the substrate inhibition effect. The mutant W490A may be ideal for industrial application due to its high yield, no substrate inhibition and high catalytic activity and pH/temperature stability. To the best of our knowledge, this is the first time to eliminate the substrate inhibition effect of glycoside hydrolase by protein engineering.

2. Materials and methods

2.1. Molecular cloning

Construction of the expression vector plasmids of OfHex1 and its mutants (V327G, E328Q, E328A, Y471V, V484R, W490A and W490H) were conducted as described previously [11]. Mutations of OfHex1 were made by In-Fusion Advantage PCR Cloning Kit (TaKaRa, China) using the following primers: V327G (5′-GGTGAGCCCCCATGCGGTCAGCTC-3′ and 5′-CGCATGGGGGCTCACCGCAGTATGATTTCC-3′); E328Q (5′-CAGCCCCCATGCGGTCAGCTCA-3′ and 5′-ACCGCATGGGGGCTGCACGCAG-3′); E328A (5′-GCGCCCCCATGCGGTCAGCTCA-3′ and 5′-ACCGCATGGGGGCGCCACGCAG-3′); Y471V (5′-CAACCATTGTTCTCCTTACAT-3′ and 5′-GGAGAACAATGGTTGTTACCAGCGCCGA-3′); V484R (5′-AGAGGCGCTGGTAACAACTGGTGTTC-3′ and 5′-TGTTACCAGCGCCTCTCCACGCTCCGAAGCC-3′); W490A (5′-GCTTGTTCTCCTTACATCGGATGGCAG-3′ and 5′-GATGTAAGGAGAACAAGCGTTGTTACCAGC-3′); W490H (5′-CAACCATTGTTCTCCTTACAT-3′ and 5′-GGAGAACAATGGTTGTTACCAGCGCCGA-3′). Two three-point mutants including V327G/V484R/W490A and V327G/Y471V/W490H were also prepared using the primers mentioned above. Then the expression vector plasmids were linearized by *Pme*I (New England Biolabs, China) and transformed into *P. pastoris* GS115 cells by electroporation. After growing on a RDB plate at 30 °C for 48 h, the positive clones were selected by PCR.

The coding region of chitobiase from *Serratia marcescens* (SmChb) was amplified from the genomic DNA of *S. marcescens* 21537 (China Center of Industrial Culture Collection, China) by PCR using forward primer 5′-AGGAGATATACCATG**CATCATCATCATCATCAT**AACGCATTCAAACTGAGCGCGCTTG-3′ and reverse primer 5′-GACGGAGCTCGAATTCTAGACCTTCTCGGCGCGGCTGTA-3′. N-terminal 6 × His-tag (in bold) were introduced through PCR. Gene encoding SmChb with N-terminal 6 × His-tag was ligated with *Noc*I/*Eco*RI-digested pET28(α) + vector (Merck, China) using In-Fusion™ Advantage PCR Cloning Kit (TaKaRa) according to the manufacturer's instructions. The resulting expression plasmid vector pET28-SmChb was transformed into *Escherichia coli* strain BL21 (DE3) and the transformants were selected by growing on LB medium with kanamycin (50 μg/mL).

2.2. Expression and purification of recombinant enzymes

The expression and purification of wild-type and mutant OfHex1 were performed as described previously [11]. The positive clones were cultured in BMMY medium at 30 °C for 144 h, and methanol (1% of the total volume) was added every 24 h. Wild-type and mutant OfHex1 were purified from the culture supernatant by ammonium sulphate precipitation (65% saturation), affinity chromatography on a HisTrap HP column (5 mL, GE Healthcare, China) followed by anion exchange chromatography on a Mono Q 5/50 GL column (1 mL, GE Healthcare, China) [11].

E. coli BL21 (DE3) cells transformed with pET28-SmChb were grown in LB medium containing 50 μg/mL kanamycin at 37 °C with shaking speed of 180 rpm until the OD_{600} reached 0.60. Expression of the recombinant SmChb was induced by the addition of IPTG to a final concentration of 0.5 mM. The cells were incubated for another 6 h at 30 °C with a shaking speed of 180 rpm. Then the cells were collected by centrifugation at 8000 rpm for 10 min and resuspended in buffer A (20 mM sodium phosphate, 0.5 M NaCl, pH 7.4). After cell disruption by high-pressure homogenizer (ATS Engineering, Canada), cell debris was removed by centrifugation at 8000 rpm for 10 min and the supernatant was loaded onto a HisTrap HP column (5 mL) pre-equilibrated with buffer A. The target protein was eluted with buffer A containing 100 mM imidazole. Then SmChb was further purified by anion exchange chromatography on a Mono Q 5/50 GL column (1 mL, GE Healthcare, China) with a linear gradient of NaCl from 0 to 250 mM.

The enzymatic activity of OfHex1, OfHex1 mutants and SmChb was assayed using *p*NP-β-GlcNAc (Sigma–Aldrich, USA) as substrate and the purity was analyzed by SDS-PAGE.

2.3. Enzymatic activity assays

Beta-*N*-acetyl-D-hexosaminidase from human placenta (HsHex) and β-*N*-acetyl-D-hexosaminidase from *Streptomyces plicatus* (SpHex) were purchased from Sigma and New England Biolabs, respectively.

For the substrate *p*NP-β-GlcNAc, the reaction mixtures contained substrate (0.05–5 mM) and appropriate mount of enzyme in 100 μL of Britton–Robinson's wide range buffer (pH 7.0 for OfHex1 and its mutants; pH 4.0 for HsHex and SpHex). After incubation at 30 °C for a specific period, the reaction was stopped by adding 100 μL of 0.5 M Na_2CO_3 and absorbance was measured at 405 nm using a Sunrise microplate reader (TECAN, Switzerland). The reaction velocity was quantified by comparing the absorbance of the product *p*NP to standard curve of *p*NP with known concentrations.

For the substrate 4-methylumbelliferyl-*N*-acetyl-β-D-glucosaminide (MU-β-GlcNAc, Sigma–Aldrich, USA), the reaction mixtures contained substrate (1–16 μM) and appropriate mount of enzyme in 100 μL of Britton–Robinson's wide range buffer (pH 7.0). After incubation at 30 °C for a specific period, the reaction was stopped by adding 100 μL of 0.5 M glycine–NaOH (pH 10.3) and fluorescence was measured using a microplate reader (Thermo Scientific Varioskan Flash, Thermo, USA) using excitation and emission wavelengths of 360 and 405 nm, respectively. The reaction velocity was quantified by comparing the absorbance of the product MU to standard curve of MU with known concentrations. The K_m and k_{cat} values were also calculated by linear regression of the data using Lineweaver–Burk plots.

For the substrate $(GlcNAc)_{2-4}$ (Toronto Research Chemicals, Canada). Before the assay, the buffer in which the enzyme was stored in was exchanged to 5 mM sodium phosphate buffer (pH 7.0) using a 5 mL HiTrap desalting column (GE Healthcare, China). The enzymatic reaction mixture consisted of 30 μL of $(GlcNAc)_{2-4}$ at varying concentrations in 5 mM sodium phosphate buffer, 28 μL of 5 mM sodium phosphate buffer (pH 7.0), and 2 μL of enzyme. The reaction mixtures were incubated at 25 °C for appropriate time and then the reaction was immediately stopped by incubation on ice. The hydrolysis products were analyzed by HPLC using a TSKgel Amide-80 column (4.6 mm × 250 mm, Tosoh, Japan) on an Agilent 1200 HPLC system (Agilent, USA). Ten microliters of reaction mixture was analyzed using 70% acetonitrile as the mobile phase at a flow rate of 0.7 mL/min. The eluent was monitored at 210 nm. The hydrolytic products were quantified by converting the peak area to concentration values according to standard curve of GlcNAc with known concentrations. Enzymatic reactions were terminated before 15% of substrate was consumed. The K_m and k_{cat} values were also calculated by linear regression of the data using Lineweaver–Burk plots.

2.4. pH and temperature profiles of OfHex1, W490A and SmChb

The pH and temperature stabilities of OfHex1, W490A and SmChb were performed using *p*NP-β-GlcNAc as substrate as described above. To study the pH stability, these enzymes were incubated in Britton–Robinson's wide range buffer (ranging from pH 3 to 12) for 2 h before assay. To study the thermal stability these enzymes were incubated in Britton–Robinson's wide range buffer (pH 7.0) at different temperatures from 10 °C to 70 °C for 2 h before assay.

3. Results

3.1. Substrate inhibition mechanism of OfHex1

The substrate inhibition mechanism of OfHex1 was studied by using $(GlcNAc)_2$ and *p*NP-β-GlcNAc as model substrates.

In 'transglycosylation mechanism', the product of glycoside hydrolase can re-reacts with substrate and an oligosaccharide longer than the substrate can be found. As for OfHex1, no $(GlcNAc)_n$ ($n \geq 3$) product was detected by HPLC when the concentration of $(GlcNAc)_2$ was 0.5 mM (Fig. 1A), suggesting substrate inhibition of OfHex1 is not caused by transglycosylation.

In 'second substrate binding mechanism', substrate inhibition is caused by a second molecule of substrate binding to the Michaelis complex of the enzyme to form a ternary complex that reduces activity [18]. This kind of inhibition is generally described by a modified Michaelis–Menten equation,

$$v = \frac{V_{max}[S]}{K_m + [S] + (K_m[S]^2/K_{is})},$$

where [*S*] is substrate concentration, V_{max}, K_m and K_{is} are constants representing for maximum velocity, Michaelis constant

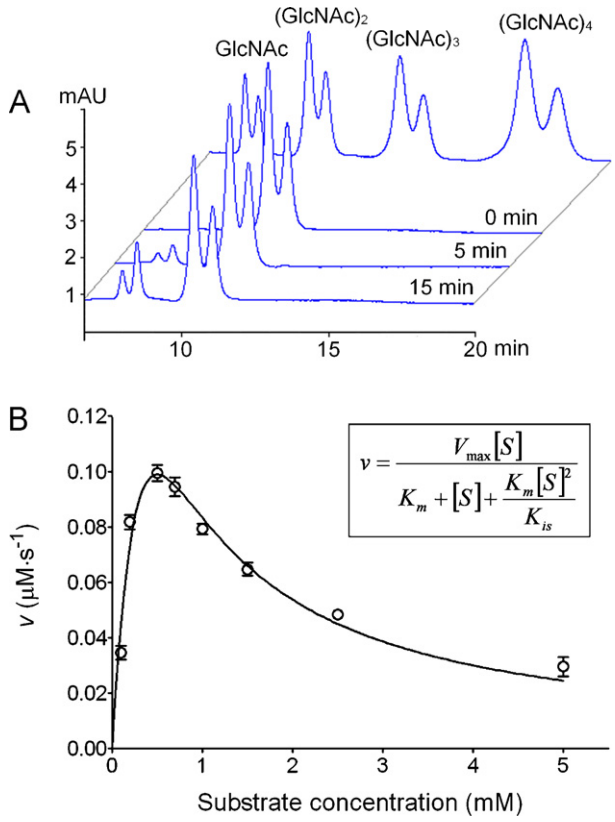

Fig. 1. Substrate inhibition of OfHex1. (A) HPLC analysis of hydrolysis products using $(GlcNAc)_2$ as substrate in the presence of OfHex1. (B) Nonlinear fitting of the substrate *p*NP-β-GlcNAc concentration vs. velocity plot to the equation of 'second substrate binding'. The experimental data were indicated by open circles and the fitted curve was indicated by lines.

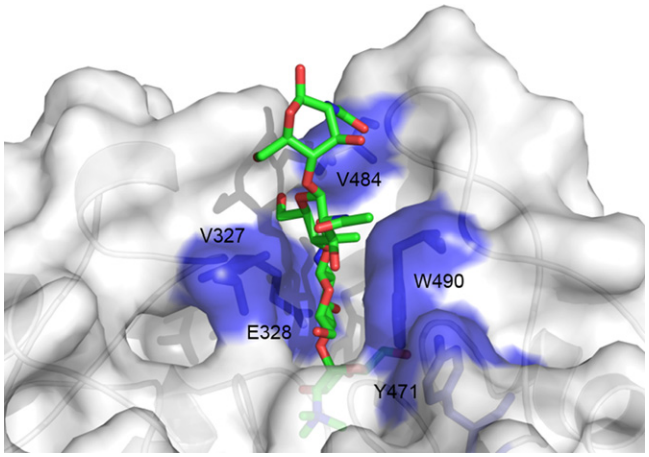

Fig. 2. Surface representation of the entrance of OfHex1's active pocket. The amino acid residues studied by site-directed mutagenesis are highlighted in blue. (For interpretation of the references to color in this figure legend, the reader is referred to the web version of the article.)

and substrate inhibition constant, respectively. As for OfHex1, the concentration of the substrate *p*NP-β-GlcNAc vs. reaction velocity are well correlated with the modified Michaelis–Menten equation with a correlation coefficient factor $R^2 = 0.956$ by nonlinear fit using Prism (GraphPad, USA) (Fig. 1B). The K_{is} value was determined to be 0.327 mM. This result demonstrated substrate inhibition of OfHex1 is caused by the second substrate binding.

In addition, the hydrolytic product, GlcNAc, was also investigated to know if product inhibition existed. The result indicated GlcNAc act as a competitive inhibitor with a K_i value of 12.5 mM. This result demonstrated that the substrate instead of product inhibition is the main issue during chitooligosaccharides hydrolysis.

3.2. Structure analysis and mutations

OfHex1 and other GH20 β-*N*-acetyl-D-hexosaminidases have highly conserved active sites. Several residues have been revealed to be vital for either catalysis or substrate binding [19–22]. In order to find out the structural basis for the "second substrate binding" mechanism, our attention was focused on the residues around the entrance of the active pocket of OfHex1. The entrance is comprised of three hydrophobic walls. As shown in Fig. 2, the left wall is composed by residues V327 and E328 and the right wall is composed by residues Y471 and W490. These two walls firmly sandwich the sugar ring of the substrate by hydrophobic interactions. However, the back wall, relatively away from the substrate binding, is composed by residues W322, W483 and V484. W322 and W483 are highly conserved among insect β-*N*-acetyl-D-hexosaminidases, whereas V484 is found in chitinolytic β-*N*-acetyl-D-hexosaminidases. By amino acid sequence alignment, an Arg residue is found to replace V484 in N-glycan modifying β-*N*-acetyl-D-hexosaminidases (Fdls) (Fig. S1). This change of a hydrophobic residue (Val) to a hydrophilic one (Arg) is interesting because the back wall faces the polar groups of the substrate. In addition, no substrate inhibition has been known for Fdls [23]. Thus, five residues including V327, E328, Y471, V484 and W490 were mutated to the corresponding conserved residues in Fdls, namely Gly, Gln/Ala, Val, Arg and Ala/His, respectively. Moreover, two sets of triple-site mutagenesis (V327G/V484R/W490A and V327G/Y471V/W490H) were also designed to test the combined effects.

Supplementary material related to this article found, in the online version, at http://dx.doi.org/10.1016/j.procbio.2012.11.018.

3.3. Expression, purification and characterization of OfHex1 mutants

Nine mutants of OfHex1 [V327G, E328Q, E328A, Y471V, V484R, W490A, W490H, V327G/V484R/W490A and V327G/Y471V/W490H] were constructed. The yield was determined by western blot analysis using His·Tag monoclonal antibody or by activity assay using synthesized substrate, *p*NP-β-GlcNAc, as substrate. Activity testing indicated that there was no activity detectable for the mutants Y471V and W490H. And western blot confirmed that the expression of these two mutants failed. Around 5–7 mg purified recombinant enzymes including V327G, E328Q, E328A and W490A were obtained from 1 L of culture medium. While, only around 0.2–0.5 mg/L of mutant enzymes were obtained, which included V484R, V327G/V484R/W490A and V327G/Y471V/W490H.

The effects of substrate concentration on these mutant enzymes were compared using *p*NP-β-GlcNAc as substrate. As shown in Fig. 3, mutation of V327, E328, Y471, V484 and W490 obviously affected the OfHex1's sensibility to the substrate concentration. The maximum velocity of E328Q and E328A could be reached at the substrate concentration of 0.5 mM (Fig. 3A). However, the maximum velocity of V327G could be reached at the substrate concentration of 0.2 mM (Fig. 3A). Interestingly, mutant enzymes including V484R, W490A, V327G/V484R/W490A and V327G/Y471V/W490H were not affected by the substrate concentration in the range of 0–2.5 mM (Fig. 3B). The enzyme W490A was the best-performing

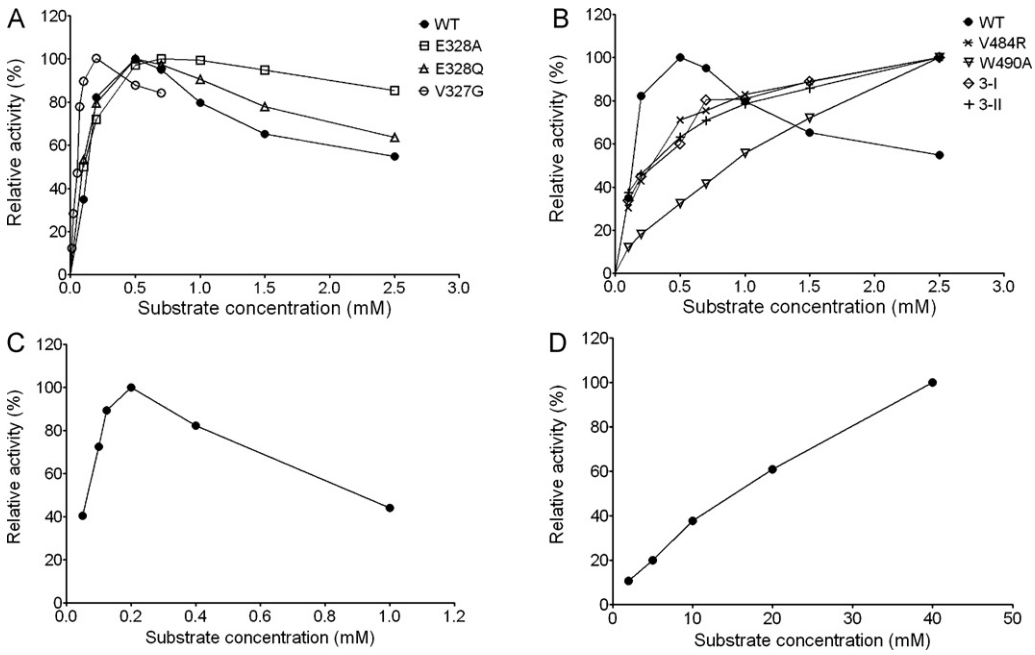

Fig. 3. Effects of substrate concentrations on the activities of the wild-type OfHex1 and its mutants. (A) Effects of the concentration of *p*NP-β-GlcNAc on the activities of the wild-type, V327G, E328A and E328Q. (B) Effects of the concentration of *p*NP-β-GlcNAc on the activities of the wild-type, V484R, W490A, V327G/V484R/W490A and V327G/Y471V/W490H. (C, D) Effects of the concentration of $(GlcNAc)_2$ on the activities of the wild-type and W490A.

one because its $v/[S]$ curve was closest to a straight line. By using natural substrate, $(GlcNAc)_2$, the inhibition concentration of $(GlcNAc)_2$ was above 0.2 mM for the wild-type (Fig. 3C), whereas for W490A, there was no inhibition observed even when the concentration of $(GlcNAc)_2$ reached at 40 mM (Fig. 3D).

Then the catalytic efficiencies of these mutants were compared using MU-β-GlcNAc as substrate. MU-β-GlcNAc was selected for its high sensitivity, thus lower substrate concentrations ($\leq$16 μM) can be used to avoid substrate inhibition effect. Except two triple-site mutations, the single site mutants have little effects on the K_m values but significant effects on the k_{cat} values (Table 1). As demonstrated by the k_{cat}/K_m values, W490A, V327G, E328Q and E328A retain activities with the same order of magnitude (10^3) as the wild-type, whereas the V484R, V327G/V484R/W490A and V327G/Y471V/W490H exhibited much lower activities (with k_{cat}/K_m values ranging from 10 to 10^2) than the wild-type (Table 1). Thus, the W490A could be evaluated as the most promising β-*N*-acetyl-D-hexosaminidase due to the high yield, no substrate inhibition and the high catalytic activity. Although both W490A and V327G/V484R/W490A contain the mutation of Trp490 to Ala490, the k_{cat}/K_m value for the V327G/V484R/W490A is rather low, perhaps suggesting synergetic effects occur among the three residues.

Table 1
Kinetic parameters of OfHex1 and its mutants using MU-β-GlcNAc as substrate.

Enzyme	K_m (mM)	k_{cat} (s^{-1})	k_{cat}/K_m (s^{-1} mM^{-1})
WT	0.101 ± 0.007	430.2 ± 10.7	4259
V327G	0.073 ± 0.003	192.1 ± 3.5	2632
E328Q	0.102 ± 0.005	351.3 ± 7.4	3444
E328A	0.096 ± 0.004	317.2 ± 6.5	3304
V484R	0.095 ± 0.008	92.5 ± 2.0	974
W490A	0.100 ± 0.004	174.6 ± 3.6	1746
W490H	ND	ND	ND
Y471V	ND	ND	ND
V327G/V484R/W490A	0.042 ± 0.002	1.4 ± 0.1	33
V327G/Y471V/W490H	0.036 ± 0.003	7.4 ± 0.2	483

3.4. Application of W490A in chitooligosaccharides degradation

Various experiments were performed to evaluate whether the protein engineered W490A is suitable as a biocatalyst for chitooligosaccharides degradation.

First, we evaluated the catalytic kinetics of W490A using chitooligosaccharides $(GlcNAc)_{2-4}$. *S. marcescens* is a potent chitinolytic bacterium and its chitinases (SmChiA, SmChiB and SmChiC) and β-*N*-acetyl-D-hexosaminidase (SmChb) have been well studied [24,25]. Here, SmChb was applied to be compared with W490A. As indicated by the k_{cat}/K_m values, OfHex1, W490A and SmChb seemed to prefer shorter chitooligosaccharides (Table 2). Though the K_m values decreased as the lengths of chitooligosaccharides increased, the k_{cat} values dropped more quickly. Though the K_m values were significantly changed by the mutation of W490 to A490, the k_{cat} values were slightly changed. Compared to the SmChb, W490A was a more efficient enzyme according to the higher k_{cat} values. Similar as the wild-type OfHex1, SmChb also encountered substrate inhibition when the concentration of synthesized substrate, *p*NP-β-GlcNAc, was above 0.7 mM (Fig. 5).

Considering the industrial application, both the pH and temperature stability were studied. As shown in Fig. 4A, either the wild-type or the mutant W490A was more stable than SmChb at acidic pHs (pH 4–6), while the mutant W490A is relatively less stable in basic pHs (8–11) but still exhibited high activity at pH 11.

The W490A remained activity after incubation at 50 °C for 2 h, meaning it was more stable than SmChb but less stable than the wild-type (Fig. 4B).

3.5. Substrate inhibition of structure-known β-*N*-acetyl-D-hexosaminidases

The effects of substrate concentration on structure-known enzymes including the bacterial β-*N*-acetyl-D-hexosaminidases (SmChb and SpHex) and the human β-*N*-acetyl-D-hexosaminidase

Table 2
Comparison of kinetic parameters of OfHex1, OfHex1–W490A and SmChb using chitooligosaccharides $(GlcNAc)_{2-4}$ as substrates.

Substrate	OfHex1		OfHex1–W490A		SmChb	
	K_m (mM)	k_{cat} (s^{-1})	K_m (mM)	k_{cat} (s^{-1})	K_m (mM)	k_{cat} (s^{-1})
$(GlcNAc)_2$	0.148 ± 0.003	507.4 ± 3.7	1.875 ± 0.042	449.6 ± 19.8	0.501 ± 0.062	284.2 ± 11.3
$(GlcNAc)_3$	0.070 ± 0.002	212.0 ± 3.3	1.554 ± 0.076	173.0 ± 3.4	0.113 ± 0.021	48.3 ± 1.6
$(GlcNAc)_4$	0.057 ± 0.001	45.4 ± 1.4	0.585 ± 0.023	46.7 ± 2.4	0.074 ± 0.002	13.1 ± 0.3

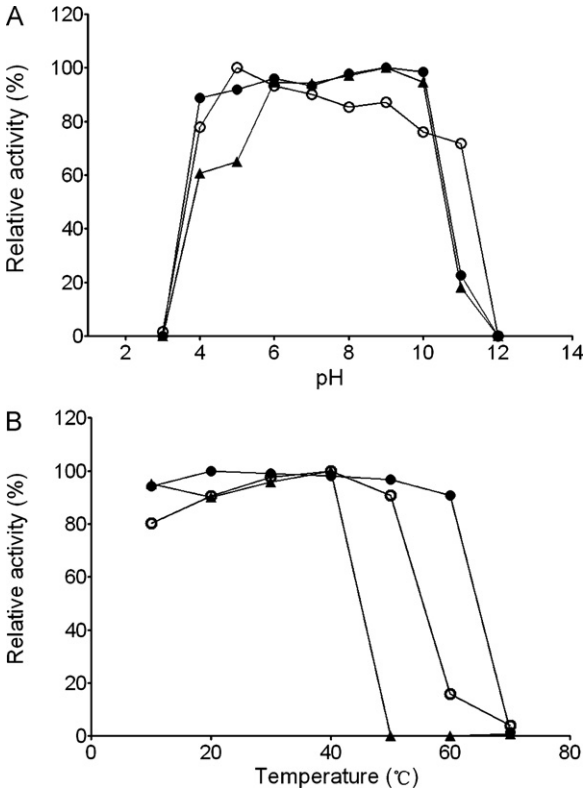

Fig. 4. pH and temperature stabilities of the wild-type OfHex1(in filled circle), W490A (in open circle) and SmChb (in filled triangle). (A) pH stabilities of wild-type OfHex1, W490A mutant and SmChb. (B) Temperature stabilities of wild-type OfHex1, W490A mutant and SmChb.

(HsHex) were investigated using *p*NP-β-GlcNAc as substrate [24,26–29]. As shown in Fig. 5, SmChb and SpHex encountered substrate inhibition when the substrate concentrations were higher than 0.5 mM and 0.2 mM, respectively. However, no substrate inhibition was observed for HsHex even when substrate concentration was above 5 mM.

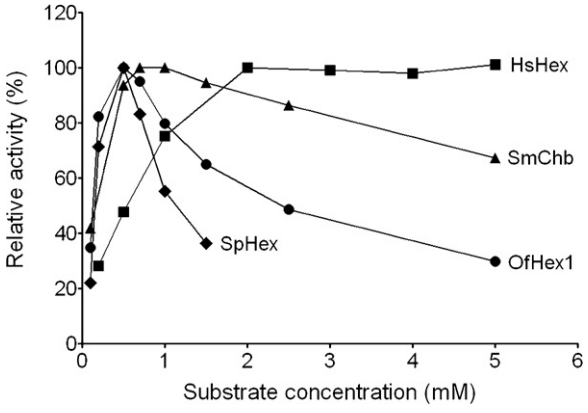

Fig. 5. Effects of the concentration of *p*NP-β-GlcNAc on the activities of the structure known β-*N*-acetyl-D-hexosaminidases.

4. Discussion

OfHex1 is a potent β-*N*-acetyl-D-hexosaminidase that can be applied in the preparation of GlcNAc. Since there are no transglycosylation products produced during OfHex1-catalyzed reaction, and the $v/[S]$ curve fitting well to the kinetic equation of the second substrate binding, the substrate inhibition of OfHex1 was via the 'second substrate binding' mechanism.

Among nine mutants of OfHex1, W490A possesses very good characteristics. First, more than 5 mg of purified W490A can be conveniently obtained from 1 L of *P. pastoris* culture medium. Second, no substrate inhibition of W490A appeared when 40 mM of $(GlcNAc)_2$ is applied (Fig. 3D). Third, W490A exhibited high catalytic activity in the same order of magnitude with the wild-type OfHex1 (Table 1) and high pH/temperature stability (Fig. 4). Moreover, W490A outperforms SmChb (the well studied bacterial β-*N*-acetyl-D-hexosaminidase) in the aspect of k_{cat} values for $(GlcNAc)_{2-4}$ as substrate (Table 2) and pH/temperature stability (Fig. 4). Thus, W490A may be an ideal β-*N*-acetyl-D-hexosaminidase for enzymatic preparation of GlcNAc.

The recently revealed crystal structure of OfHex1 allowed us to find the structural basis of substrate inhibition [22]. The amino acid residues, V327, E328, Y471, V484 and W490, were chosen due to their locations around the active pocket. V327, E328 and W490 directly interact with the +1 GlcNAc via hydrophobic and polar interactions while Y471 and V484 are important residues comprising the hydrophobic wall of the active pocket (Fig. 2). Site-directed mutagenesis experiments showed that two single-site mutants (V484R and W490A) and two triple-site mutants (V327G/V484R/W490A and V327G/Y471V/W490H) lessened substrate inhibition of OfHex1 whereas the best performing mutant is W490A. The direct consequence of the replacement of indolyl

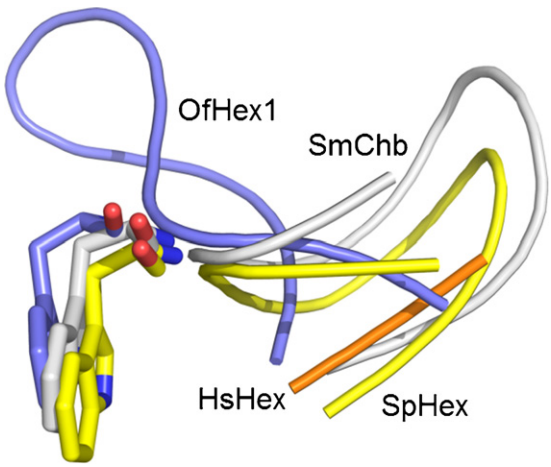

Fig. 6. Structural alignment of the conserved Trp residues and the corresponding loops in OfHex1 (blue), SmChb (white), SpHex (yellow) and HsHex (orange). (For interpretation of the references to color in this figure legend, the reader is referred to the web version of the article.)

side chain (W490) to methyl side chain (A490) is the loss of the hydrophobic interactions with +1 GlcNAc. By structure-based sequence alignment, other chitinolytic enzymes including bacterial SmChb and SpHex, both of which exhibit substrate inhibition (Fig. 5), also has this conserved Trp (W685 in SmChb and W408 in SpHex) (Fig. 6). This Trp is located in extended loops between strand β7 and β8 of the $(\alpha/\beta)_8$-barrel catalytic domains whereas the corresponding loop in HsHex, whose activity not affected by substrate inhibition, is very short (Fig. 6) [27,28]. So, we believe that the residue W490 determines the second substrate binding by its bulky side chain.

Acknowledgments

The authors acknowledge the financial support provided by the National Key Project for Basic Research (2010CB126100), the National Natural Science Foundation of China (31070715, 31101671), the National High Technology Research and Development Program of China (2011AA10A204), the National Key Technology R&D Program (2011BAE06B05), the Fundamental Research Funds for the Central Universities (DUT11ZD113, DUT11RC(3)73).

References

[1] Tharanathan RN, Kittur FS. Chitin – the undisputed biomolecule of great potential. Crit Rev Food Sci 2003;43:61–87.
[2] Tamai Y, Miyatake K, Okamoto Y, Takamori Y, Sakamoto K, Minami S. Enhanced healing of cartilaginous injuries by N-acetyl-D-glucosamine and glucuronic acid. Carbohyd Polym 2003;54:251–62.
[3] Salvatore S, Heuschkel R, Tomlin S, Davies SE, Edwards S, Walker-Smith JA, et al. A pilot study of N-acetyl glucosamine, a nutritional substrate for glycosaminoglycan synthesis, in paediatric chronic inflammatory bowel disease. Aliment Pharmacol Ther 2000;14:1567–79.
[4] Chen JK, Shen CR, Liu CL. N-Acetylglucosamine: production and applications. Mar Drugs 2010;8:2493–516.
[5] Bissett DL, Robinson LR, Raleigh PS, Miyamoto K, Hakozaki T, Li J, et al. Reduction in the appearance of facial hyperpigmentation by topical N-acetyl glucosamine. J Cosmet Dermatol 2007;6:20–6.
[6] Binod P, Sandhya C, Suma P, Szakacs G, Pandey A. Fungal biosynthesis of endochitinase and chitobiase in solid state fermentation and their application for the production of N-acetyl-D-glucosamine from colloidal chitin. Bioresour Technol 2007;98:2742–8.
[7] Dahiya N, Tewari R, Hoondal GS. Biotechnological aspects of chitinolytic enzymes: a review. Appl Microbiol Biotechnol 2006;71:773–82.
[8] Sashiwa H, Fujishima S, Yamano N, Kawasaki N, Nakayama A, Muraki E, et al. Production of N-acetyl-D-glucosamine from β-chitin by enzymatic hydrolysis. Chem Lett 2001:308–9.
[9] Cederkvist FH, Parmer MP, Varum KM, Eijsink VGH, Sorlie M. Inhibition of a family 18 chitinase by chitooligosaccharides. Carbohyd Polym 2008;74:41–9.
[10] Yang Q, Liu T, Liu FY, Qu MB, Qian XH. A novel β-N-acetyl-D-hexosaminidase from the insect *Ostrinia furnacalis* (Guenee). FEBS J 2008;275:5690–702.
[11] Liu T, Liu FY, Yang Q, Yang J. Expression, purification and characterization of the chitinolytic β-N-acetyl-D-hexosaminidase from the insect *Ostrinia furnacalis*. Protein Expr Purif 2009;68:99–103.
[12] Schomburg I, Chang AJ, Hofmann O, Ebeling C, Ehrentreich F, Schomburg D. BRENDA: a resource for enzyme data and metabolic information. Trends Biochem Sci 2002;27:54–6.
[13] Reed MC, Lieb A, Nijhout HF. The biological significance of substrate inhibition: a mechanism with diverse functions. Bioessays 2010;32:422–9.
[14] Andric P, Meyer AS, Jensen PA, Dam-Johansen K. Reactor design for minimizing product inhibition during enzymatic lignocellulose hydrolysis: I. Significance and mechanism of cellobiose and glucose inhibition on cellulolytic enzymes. Biotechnol Adv 2010;28:308–24.
[15] Chou YT, Yao SH, Czerwinski R, Fleming M, Krykbaev R, Xuan DJ, et al. Kinetic characterization of recombinant human acidic mammalian chitinase. Biochemistry 2006;45:4444–54.
[16] Singh S, Gallagher R, Derrick PJ, Crout DHG. Glycosidase-catalyzed oligosaccharide synthesis – preparation of the N-acetylchitooligosaccharides penta-N-acetylchitopentaose and hexa-N-acetylchitohexaose using the β-N-acetylhexosaminidase of *Aspergillus oryzae*. Tetrahedron: Asymmetry 1995;6:2803–10.
[17] Ryslava H, Kalendova A, Doubnerova V, Skocdopol P, Kumar V, Kukacka Z, et al. Enzymatic characterization and molecular modeling of an evolutionarily interesting fungal β-N-acetylhexosaminidase. FEBS J 2011;278:2469–84.
[18] Mayer C, Zechel DL, Reid SP, Warren RAJ, Withers SG. The E358S mutant of *Agrobacterium* sp. β-glucosidase is a greatly improved glycosynthase. FEBS Lett 2000;466:40–4.
[19] Mark BL, Wasney GA, Salo TJS, Khan AR, Cao ZM, Robbins PW, et al. Structural and functional characterization of *Streptomyces plicatus* β-N-acetylhexosaminidase by comparative molecular modeling and site-directed mutagenesis. J Biol Chem 1998;273:19618–24.
[20] Prag G, Papanikolau Y, Tavlas G, Vorgias CE, Petratos K, Oppenheim AB. Structures of chitobiase mutants complexed with the substrate di-N-acetyl-D-glucosamine: the catalytic role of the conserved acidic pair, aspartate 539 and glutamate 540. J Mol Biol 2000;300:611–7.
[21] Manuel SGA, Ragunath C, Sait HBR, Izano EA, Kaplan JB, Ramasubbu N. Role of active-site residues of dispersin B, a biofilm-releasing β-hexosaminidase from a periodontal pathogen, in substrate hydrolysis. FEBS J 2007;274:5987–99.
[22] Liu T, Zhang HT, Liu FY, Wu QY, Shen X, Yang Q. Structural determinants of an insect β-N-acetyl-D-hexosaminidase specialized as a chitinolytic enzyme. J Biol Chem 2011;286:4049–58.
[23] Leonard R, Rendic D, Rabouille C, Wilson IBH, Preat T, Altmann F. The Drosophila fused lobes gene encodes an N-acetylglucosaminidase involved in N-glycan processing. J Biol Chem 2006;281:4867–75.
[24] Tews I, Perrakis A, Oppenheim A, Dauter Z, Wilson KS, Vorgias CE. Bacterial chitobiase structure provides insight into catalytic mechanism and the basis of Tay-Sachs disease. Nat Struct Biol 1996;3:638–48.
[25] Horn SJ, Sorlie M, Vaaje-Kolstad G, Norberg AL, Synstad B, Varum KM, et al. Comparative studies of chitinases A, B and C from *Serratia marcescens*. Biocatal Biotransform 2006;24:39–53.
[26] Mark BL, Vocadlo DJ, Knapp S, Triggs-Raine BL, Withers SG, James MNG. Crystallographic evidence for substrate-assisted catalysis in a bacterial β-hexosaminidase. J Biol Chem 2001;276:10330–7.
[27] Maier T, Strater N, Schuette CG, Klingenstein R, Sandhoff K, Saenger W. The X-ray crystal structure of human β-hexosaminidase B provides new insights into Sandhoff disease. J Mol Biol 2003;328:669–81.
[28] Mark BL, Mahuran DJ, Cherney MM, Zhao DL, Knapp S, James MNG. Crystal structure of human β-hexosaminidase B: understanding the molecular basis of Sandhoff and Tay-Sachs disease. J Mol Biol 2003;327:1093–109.
[29] Lemieux MJ, Mark BL, Cherney MM, Withers SG, Mahuran DJ, James MNG. Crystallographic structure of human β-hexosaminidase A: interpretation of Tay-Sachs mutations and loss of GM2 ganglioside hydrolysis. J Mol Biol 2006;359:913–29.